SPATIAL HETEROGENEITY OF PHYLOGENETICALLY DIVERSE ORANGE AND WHITE *BEGGIATOA* MATS IN GUAYMAS BASIN HYDROTHERMAL SEDIMENTS

Luke Justin McKay

A thesis submitted to the faculty of the University of North Carolina at Chapel Hill in partial fulfillment of the requirements for the degree of Master of Science in the Department of Marine Sciences.

Chapel Hill
2011

Approved by:

Dr. Andreas Teske

Dr. Barbara MacGregor

Dr. Carol Arnosti

ABSTRACT

LUKE MCKAY: Spatial Heterogeneity of Phylogenetically Diverse Orange and White *Beggiatoa* Mats in Guaymas Basin Hydrothermal Sediments
(Under the direction of Dr. Andreas Teske)

Sulfide-oxidizing bacteria of the genus *Beggiatoa* form colorful mats on the seafloor above active hydrothermal seeps at Guaymas Basin. 113 temperature profiles were taken around 15 *Beggiatoa* mats to investigate spatial relationships between mat color and hydrothermal seeps. Average *in situ* temperatures of phylogenetically diverse orange and white filaments are 8-12°C, indicating that Guaymas *Beggiatoa* live in relatively cool conditions. Average temperatures 40 centimeters beneath all *Beggiatoa* mats are approximately 90°C. Orange filaments are usually concentrated over hotter subsurface temperatures in the center of a mat than the major concentration of white filaments at the periphery; however, the range of subsurface temperatures changes from one mat to another. Elevated temperature profiles beneath orange *Beggiatoa* correlate with the shallowest sulfide accumulation maxima. We propose that spatial heterogeneity of orange and white filaments in a Guaymas *Beggiatoa* mat is controlled by delivery of, and proximity to, energy sources in the shallow subsurface.

To The D:
Donald Trad Nogueira-Godsey, Marvin Lionel Leathers, Kyle Douglass Jones,
Stephen Andrew Sansom, James Allison King, John Zachary Sullivan,
and William Augustus McMurray IV

ACKNOWLEDGEMENTS

This study would not have been possible without extensive input and support from Andreas Teske, Barbara MacGregor, Daniel Albert, Daniel Hoer, Howard Mendlovitz, Jennifer Biddle, and Julius Lipp. I am very grateful for guidance and suggestions given by my advisory committee: Carol Arnosti, Barbara MacGregor, and Andreas Teske. I would like to thank the crews of the R/V *Atlantis* and HOV *Alvin* for their outstanding efforts and constant ability to solve problems during the dives in Guaymas Basin. I thank all shipboard scientists for their willingness to contribute ideas and time to this investigation. Additionally, I am indebted to Andrea Anton, Patrick Gibson, Brian White, and Hans Røy for helpful discussion. Figure 2 was constructed by Julius Lipp with help from Barbara MacGregor and myself. This study was funded by the National Science Foundation (Biological Oceanography 0647633) and I was funded in part by the Graduate School Science and Technology Fellowship from UNC-Chapel Hill. Lastly, I thank the Department of Marine Sciences and my advisor, Andreas Teske, for giving me the opportunity to conduct very fun oceanographic research.

TABLE OF CONTENTS

LIST OF TABLES.....vi

LIST OF FIGURES.....vii

Chapter

I. INTRODUCTION.....1

II. SPATIAL HETEROGENEITY OF PHYLOGENETICALLY DIVERSE ORANGE AND WHITE *BEGGIATOA* MATS IN GUAYMAS BASIN HYDROTHERMAL SEDIMENTS.....4

Sampling Procedures and Methodology.....4

Results and Discussion.....8

Conclusion.....21

APPENDIX.....22

REFERENCES.....31

LIST OF TABLES

Table

1. Guaymas Basin *Beggiatoa* mat temperature profiles.....Appendix I

LIST OF FIGURES

Figure

1. 16S phylogenetic tree incorporating six Guaymas *Beggiatoa* filaments....8

2. Three-dimensional reconstruction of MegaMat temperature fields....10

3. Average surface and deep temperatures grouped by mat color or presence....11

4. Individual surface temperatures from orange and white mats....13

5. Temperature, sulfate, and sulfide profiles from four orange and white mats....16

LIST OF ABBREVIATIONS

C	Celsius
CM	Centimeter
CMBSF	Centimeters below seafloor
M	Meter
SPP.	Species

CHAPTER I

INTRODUCTION

Hydrothermal activity at spreading centers is typically found in open ocean regions with very low sedimentation rates. The Guaymas Basin in the Gulf of California is a unique spreading center in that hydrothermal fluids rise through a 300-400 m layer of pelagic and terrigenous organic-rich sediments before escaping at the seafloor (Einsele et al., 1980). Hydrothermal fluids that seep through the thick sediment layer can reach subsurface temperatures greater than 300°C (Edmond and Von Damm, 1985). The upward transport of methane, organic acids, hydrogen, carbon dioxide, ammonia, and hydrogen sulfide in hydrothermal flow supplies metabolic substrates to a highly diverse microbial community carrying out metabolic processes such as methanogenesis, methane oxidation, nitrification, sulfate reduction, and sulfide oxidation (Dhillon et al. 2003, 2005; Teske et al. 2002, 2009).

Beggiatoa spp. are mat-forming, filamentous, sulfide-oxidizing bacteria that colonize the surface of sulfide-rich sediments. With filament and cell diameters of up to 200 micrometers (μm), they are among the largest prokaryotes (Schulz and Jørgensen, 2001). At Guaymas Basin, *Beggiatoa* filaments range from only a few μm to more than 100 μm in diameter (Jannasch et al., 1989; Nelson et al., 1989). The intracellular volume of Guaymas *Beggiatoa* cell is taken up almost entirely by a large vacuole, while the

cytoplasm is only a thin layer between the vacuole and cell membrane (Jannasch et al., 1989; Nelson et al., 1989). In most cases, these large vacuoles accumulate and store nitrate (NO_3^-) (McHatton et al., 1996), although exceptions are known (Kalanetra et al., 2004). The thin cytoplasmic layer sometimes contains globules of elemental sulfur, and these, along with stored NO_3^- in the vacuoles, likely sustain filaments during periods of inadequate electron donor and acceptor supply (Jannasch et al., 1989; McHatton et al., 1996). In strong contrast to the brown sediments of Guaymas Basin, *Beggiatoa* spp. typically form conspicuous white, yellow, and orange mats around sites of active hydrothermal venting (Jannasch et al., 1989; Gundersen et al., 1992). The orange pigmentation in *Beggiatoa* filaments is attributed to high cytochrome content (Prince et al., 1988) based on examination of *Beggiatoa* mat sample 1615B, a suspension of brightly colored filaments of a single width class with filament diameters of mostly 25 to 35 μm (Nelson et al., 1989). The white coloration is due to the refractive nature of elemental sulfur granules stored in the cytoplasm (Schulz and Jørgensen, 2001). It is currently unclear whether the source of the yellow coloration in Beggiatoa mats is intracellular or extracellular.

The colorful *Beggiatoa* mats at the surface of otherwise brown sediments are visual markers for complex subsurface microbial communities taking advantage of the electron donor supply in hydrothermal vents and hydrocarbon seeps (Lloyd et al., 2010). *Beggiatoa* mats with both white and orange filaments show a consistent pattern: orange *Beggiatoa* spp. are found in the center of the mat at higher concentrations than white filaments, which are most concentrated at the mat periphery around the orange filaments. This spatial heterogeneity of *Beggiatoa* filament colors is seen in hot Guaymas Basin

sediments as well as cold Gulf of Mexico sediments (Larkin and Henk, 1996; Nikolaus et al., 2003), and suggests different habitat preferences of these *Beggiatoa* types. During two R/V *Atlantis* cruises to Guaymas Basin (December 5-17, 2008; November 22 to December 6, 2009), the association of *Beggiatoa* mats with hydrothermal seepage and the habitat preferences of various *Beggiatoa* types were investigated by geochemical and microbiological characterization of sediments underneath *Beggiatoa* mats in combination with temperature measurements down to 40 cm sediment depth. In particular, temperature profiles and corresponding sulfide and sulfate gradients from mats exhibiting orange-to-white color transitions were examined to elucidate hydrothermal fluid delivery and/or tolerance associated with differently colored *Beggiatoa* spp.

CHAPTER II

SPATIAL HETEROGENEITY OF PHYLOGENETICALLY DIVERSE ORANGE AND WHITE *BEGGIATOA* MATS IN THE HYDROTHERMAL FIELDS OF GUAYMAS BASIN

Sampling Procedures and Methodology

Isolation of single Beggiatoa filaments, 16S rRNA gene amplification, and phylogenetic identification.

On board the R/V *Atlantis, Beggiatoa* spp. collected either by push coring or "slurp gun" from the *Alvin* submersible were selected as single filaments with a pipette and dragged through soft agar (agarose and sterile seawater, 1:1) for about a minute before being stored at -80°C in 50 μl centrifuge tubes. Samples were then transported to the laboratory at UNC-Chapel Hill for further analysis. Full genome amplifications were performed using the Qiagen Ultra-fast miniprep genomic amplification protocol (Qiagen, Germantown, MD). From the amplified genome, the gene sequence for the 16S region of the small ribosomal RNA subunit was amplified by polymerase chain reaction (PCR) using the B8F bacterial forward primer (AGR GTT TGA TCC TGG CTC AG) and the B1492R bacterial reverse primer (CGG CTA CCT TGT TAC GAC TT) (Teske et al., 2002). PCR amplifications were run in BioRad iCycler Thermal Cycler (Hercules, CA). Each PCR reaction consisted of 1 μl amplified *Beggiatoa* genome, 2.5 μl 10X FBI buffer (TaKaRa, Shiga, Japan), 2.0 μl dNTP mix, 2.0 μl 10 μM B8F (Invitrogen, Carlsbad, CA),

2.0 µl 10 µM B1492R (Invitrogen), and 0.25 µl SpeedStar Taq polymerase (TaKaRa), and was filled to 25 µl with sterile H_2O. A preliminary melting period of 2 min at 94°C was followed by 30 cycles of the following steps: 10 sec at 98°C, 15 sec at 58°C, and 20 sec at 72°C. These cycles were followed by 5 min at 72°C and the final temperature was brought down to 12°C. Amplifications were confirmed by gel electrophoresis followed by staining with ethidium bromide and visualization under ultraviolet light. Positive samples were cloned using the TOPO TA cloning kit (Invitrogen) and individual colonies were sequenced by GeneWiz (South Plainfield, NJ).

Near-complete 16S rRNA gene sequences were analyzed using Sequencher (Gene Codes, Ann Arbor, MI) and confirmed as closely related (95% maximum identity) to other non-Guaymas *Beggiatoa* spp. via the Basic Local Alignment Search Tool (BLAST) of the National Center for Biotechnology Information (http://blast.ncbi.nlm.nih.gov/). Next, the sequences were incorporated into a 16S rRNA alignment with sequences from six closely related species of the γ-proteobacteria phylum using the ARB phylogenetic software package (Ludwig et al. 2004) and the SILVA v95 database (Pruesse et al. 2007). A phylogenetic tree was constructed using ARB's neighbor-joining function with a Jukes-Cantor correction.

Temperature profiling.

During *Alvin* dives 4483-4492 (Dec 6-17, 2008) and 4562-4573 (Nov 22-Dec 6, 2009) in the 2000 m deep Southern Guaymas trench, 113 temperature profiles were taken in sediments near and within *Beggiatoa* mats, at the hydrothermally active areas from 27°N00.30 to 27°N00.60, and 111°W24.65 to 111°W24.35. All temperature probe measurements, positions of the probe in the mat, and penetration depths were checked

with the *Alvin* dive videotapes that provide a continuous record of all dive operations. Of the 113 temperature profiles, 78 were measured in mats with both orange and white filaments to focus on the relationship between differently colored *Beggiatoa*. A Heatflow probe manufactured by the Woods Hole Oceanographic Institution (WHOI) was used to measure 69 of the 78 temperature profiles. This is a 0.6 m titanium tube containing a linear heater and five thermistors (type 44032, Omega Engineering, Inc.) at 10 cm intervals along the length of the tube (personal communication with Lane J. Abrams, WHOI). The thermistors have a tolerance of +/- 0.2 up to 40°C, and +/- 1°C up to 200°C. It is considered fully inserted when a disc at the base reaches the sediment surface, and takes temperature readings at 0, 10, 20, 30 and 40 cmbsf. For 28 profiles, 5 cm depth resolution was achieved by first inserting the probe 5cm less than complete insertion and recording one profile, and then inserting the probe the rest of the way and recording a second profile, 5 cm offset from the first. Temperatures were recorded after the readings had stabilized for each of the five depths. Occasionally, this technique resulted in channel formation, and the second set of readings was higher than the first. During dive 4490, one temperature profile was repeated three times, giving a range of sensor precisions from 1.0 to 4.1°C. A high temperature probe was used to produce nine additional temperature profiles with varying depth intervals from the sediment surface down to 37.5 cmbsf. The high temperature probe has a type-K thermocouple located at the tip, with a tolerance of +/-3°C up to 400°C. Temperature profiles with this probe were achieved by touching the tip to the sediment surface for the first reading and then inserting the probe sequentially to desired depths and taking readings.

Statistical analysis.

To analyze the relationship of sediment depth and mat color to surface and subsurface temperatures we performed a 2-way analysis of variance (ANOVA) using SigmaStat (Systat Software, San Jose, CA). Because data violated both normality and equal variance, α (2) values were reduced so that $p < 0.005$. *Post-hoc* Tukey tests were performed to estimate differences between treatment levels and the results were plotted using SigmaPlot (Systat Software, San Jose, CA). The clearest images of *Beggiatoa* mats captured by the submersible's high definition cameras were used to create maps indicating all temperature measurement locations in relation to mat cover with Adobe Photoshop CS (Adobe Systems, San Jose, CA). Two red lasers that project from *Alvin* 10 cm apart were used to create scale bars.

3-D reconstruction of temperature field.

A three-dimensional reconstruction of the temperature field below "MegaMat" (27°N0.459, 111°W24.526), the largest mat observed during the 2008 cruise, was performed based on 14 temperature profiles that were systematically collected for this location on Dive 4485 (Dec 8, 2009). Linear interpolation of measured temperature profiles between 0 cm and maximum measured depth was performed in 5 cm resolution with MatLab (The MathWorks, Natick, MA). Final temperature grids were calculated for each depth horizon using the triangle interpolation scheme of the MatLab function "gridfit" (MatLab Central, http://www.mathworks. com/matlabcentral/fileexchange/). Shorter temperature profiles that did not reach 40 cm down were not extrapolated; in such cases only data within the measured depth interval was used for calculation of the temperature grids.

Sulfate and sulfide profiles.

For porewater analyses, 15 ml Falcon tubes were filled completely with sediment; the sediment samples were centrifuged and the resulting porewater was immediately filtered using 0.45 μm syringe filters. For sulfate measurements, a 1 ml subsample was acidified with 50 μl of 50% HCl and bubbled with nitrogen for 4 minutes to remove sulfide. Sulfate analyses were performed aboard the ship using a 2010i Dionex ion chromatograph (Sunnyvale, CA), as previously described (Martens et al., 1999). A separate 1 ml porewater subsample was drawn into a syringe containing 0.1 ml of 0.1 M zinc acetate solution to preserve the sulfide as zinc sulfide until analyzed. Sulfide was analyzed spectrophotometrically aboard the ship using the Cline (1969) method.

Results and Discussion

16S rRNA gene sequences from four orange and two white Guaymas *Beggiatoa* filaments were incorporated into a phylogenetic tree with five closely related species of the phylum γ-proteobacteria (Figure 1). The six sequences represent five separate

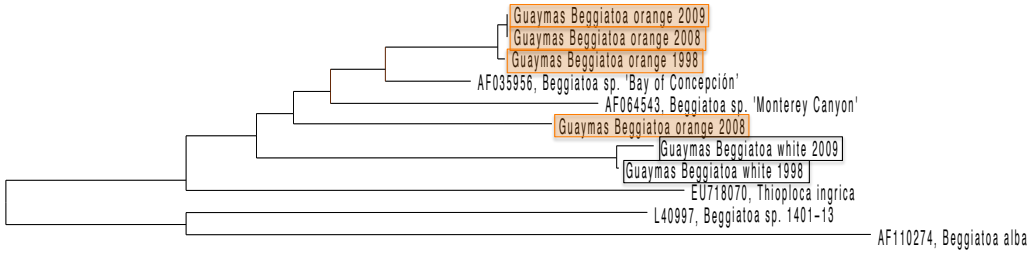

Figure 1). Phylogenetic tree based on the gene sequence for the 16S small subunit ribosomal RNA from six *Beggiatoa* filaments isolated during our two cruises to Guaymas Basin in 2008 and 2009, and another cruise in 1998. Guaymas *Beggiatoa* sequences were aligned with sequences from five closely related species of the γ-proteobacteria group. Four orange species are highlighted with orange boxes and two white species are indicated by black rectangles.

phylotypes, indicating that neither three color groups nor three size groups alone are sufficient to describe the diversity of Guaymas *Beggiatoa*. 16S rRNA sequences from

one orange filament collected on the 2008 cruise and another orange filament from 2009, both with diameters of ~25 μm, are 100% identical; however, they are only 99% and 95% similar to the other two orange *Beggiatoa* filaments collected in 1998 (35 μm filament diameter) and 2008 (diameter unknown, but less than 60 μm), respectively. The 16S rRNA sequences from the two white filaments from 1998 and 2008, both representing the 120 μm filament diameter size class (Nelson et al., 1989), are 99% identical, presenting only six base pair mismatches. The 16S rRNA gene sequences of orange and white *Beggiatoa* from Guaymas Basin reveal species-level diversity between the orange and white filaments, as well as within the orange group alone. From this analysis we propose that the change in color across a *Beggiatoa* mat is not a physiological variable within otherwise closely related or identical organisms, but marks phylogenetically distinct bacteria that sometimes overlap, but generally prefer distinct microhabitats within the same mat.

To examine the general spatial relationship between *Beggiatoa* mat cover and active hydrothermal seepage, 14 temperature profiles were taken in and around a hydrothermally active site with extensive mat cover, termed MegaMat (Dive 4485, December 8, 2008, 27°N00.464, 111°W24.512). A 3-dimensional reconstruction of MegaMat temperature profiles exhibits a characteristic feature of *Beggiatoa* mats in hydrothermally active sediments: central portions of mats have hotter surface and subsurface temperatures, which decrease considerably as temperature measurements approach bare sediments at a mat's edge (Figure 2). Surface temperatures, however, do not exceed 16.5°C, indicating that Guaymas *Beggiatoa* colonize the relatively cool sediment-water interface above hydrothermally active sediments, which reach

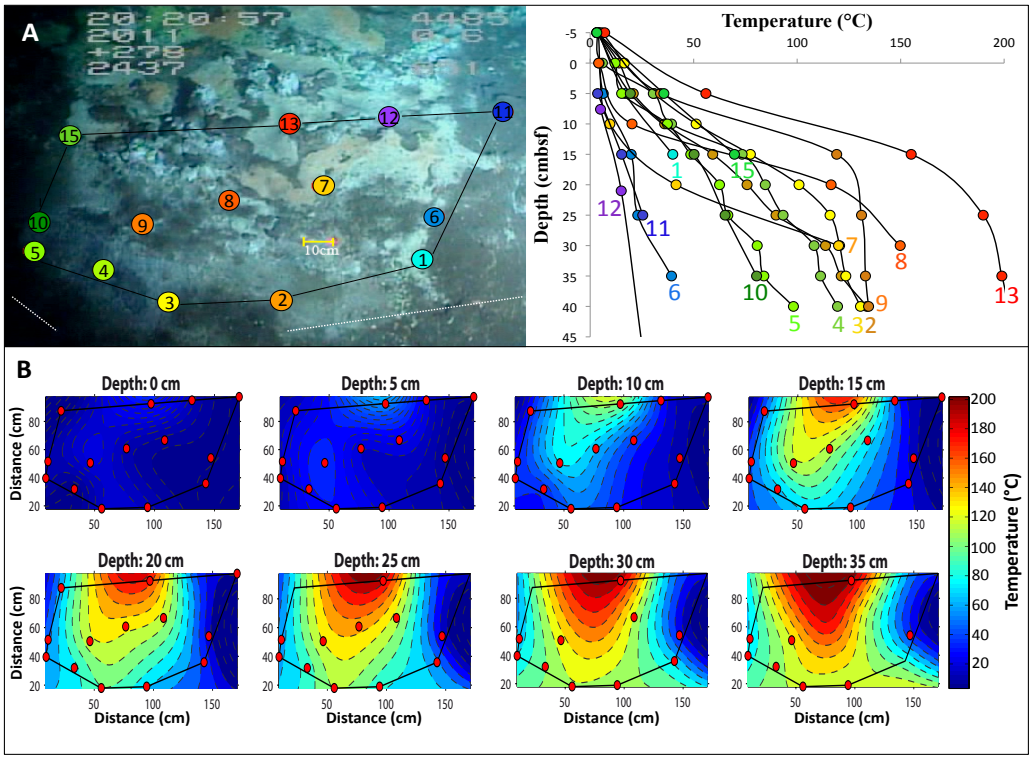

Figure 2A). MegaMat hydrothermal area with 14 color-coded temperature measurement points and their corresponding temperature profiles. **2B)** Contour plots of reconstruction of temperature field in 5 cm sediment depth intervals. Only temperature data within the measured depth interval was used for calculation of temperature grids (red dots). Short temperature profiles were not extrapolated vertically, no red dots are plotted in such cases, and temperatures at these spots were inferred based on x/y interpolation from neighboring T data points only. The black line marks the area of measured temperature data. A 10 cm scale bar is shown as the yellow line.

temperatures up to 200°C just 35 cm beneath MegaMat. To check this trend with temperature data from other Guaymas Basin locations, surface and subsurface (40 cmbsf) temperatures from 78 temperature profiles taken at 15 different mats *with both orange and white filaments* were grouped by mat color, or by distance from a mat in the case of bare sediment profiles (Figure 3). Group "O" consists of temperature profiles taken in orange portions of mats (which may have some white filaments), group "W" consists of profiles taken in white portions of mats in which no orange filaments were detected (by inspection of mat tufts with a dissection microscope), group "S" consists of profiles taken in nearby bare sediments (<1 m from a mat), and group "B" consists of profiles taken in

background sediments (>1 m from a mat). The *post hoc* Tukey test finds that depth influences temperature in groups O, W, and S (denoted by asterisks), but not in group B, which has relatively cool temperatures at every depth (Figure 3). This observation is

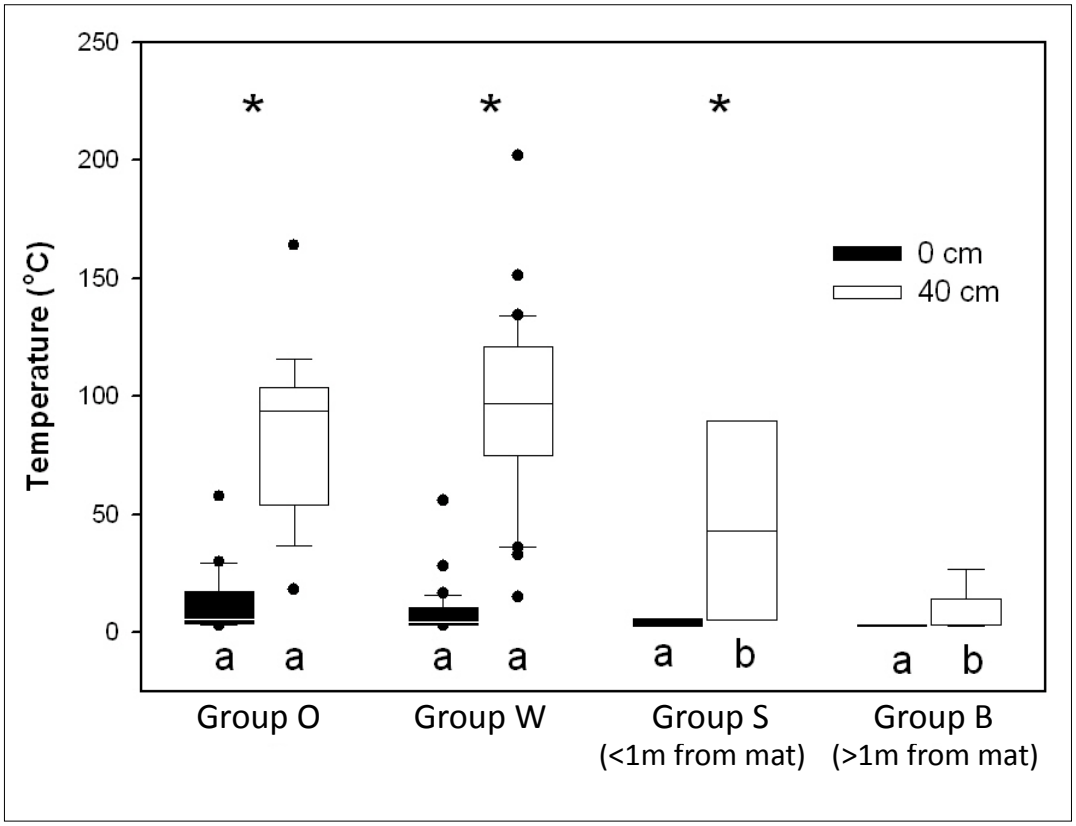

Figure 3. Box and whisker plot depicting the *in situ* temperatures for the sediment-water interface (0 cm) and 40 cm sediment depth for orange and white *Beggiatoa* mats, sediments near the mats, and cold background sediments distant from microbial mats. The boxes encompass temperature points within the 25-75th percentile range. A line through a box represents the median temperature of the group at either 0 cm or 40 cm depth. The whiskers represent the 10th percentile (at the top) and the 90th percentile (at the bottom). Points outside of the whiskers are considered outliers. The asterisks denote groups in which temperature is influenced by depth with statistical support (*post hoc* Tukey test). The letters *a* and *b* denote significant differences between group temperature averages at either 0 cm or 40 cm below seafloor. Sample sizes: Group O – 26 (0cm) and 19 (40cm); Group W – 34 (0cm) and 33 (40cm); Group S – 7 (0cm) and 6 (40cm); Group B – 8 (0cm) and 9 (40cm).

consistent with previous results that sediments unassociated with hydrothermal seepage have temperatures near the seawater background of 3°C (Gunderson et al., 1992). Surface temperatures in bare sediments near mats (group S) range from 3-7°C while background surface temperatures (group B) remain low, near 3°C. The Tukey test does not interpret

any group as encompassing significantly warmer surface temperatures than any other group. However, because all groups have a clearly defined lower limit surface temperature of 3°C set by ambient seawater conditions, and a less consistent upper limit surface temperature determined by the hydrothermal activity beneath a given mat, surface temperature averages for all groups are skewed towards 3°C. While surface temperatures within both groups O and W range from 3°C to occasionally as high as 60°C, most surface temperature measurements are in the 3-16°C range (Figure 4). This cool surface temperature range indicates that Guaymas Basin *Beggiatoa* are not thermophilic, as might be assumed from their association with hydrothermal seepage, but are associated with relatively cool *in situ* temperatures. The *in situ* temperatures of Guaymas Basin *Beggiatoa* mats are consistent with temperature optima near 20°C for CO_2 assimilation by intact *Beggiatoa* filaments (Nelson et al., 1989), and with prior *in situ* temperature sensor measurements of 3-5°C in *Beggiatoa* mats at Guaymas Basin (Gundersen et al., 1992).

The upper extent of the standard deviation from the mean of all surface temperatures from all mats is 21°C, as plotted in figure 4. Closer examination of groups O and W reveals that orange *Beggiatoa* filaments were observed at *in situ* temperatures above 21°C more often than white *Beggiatoa* filaments. If the dataset of surface temperatures from *Beggiatoa* mats is expanded to include the 28 readings in mats with only white filaments (and no orange filaments) as well as orange and white mats, the upper extent of the standard deviation changes minimally, to 22°C. High temperatures above this limit, or statistical outliers, are found in 23% of all measurements in orange sections (n=26), in contrast to either 5.9% in white sections adjacent to orange sections (n=34), or 8.1% in all white sections (n=62), including those with no nearby orange

sections. These surface temperature outliers suggest that temporary surges in hydrothermal flux might be more common beneath the predominantly orange center of a mat than the white periphery; as a corollary, orange *Beggiatoa* may have developed

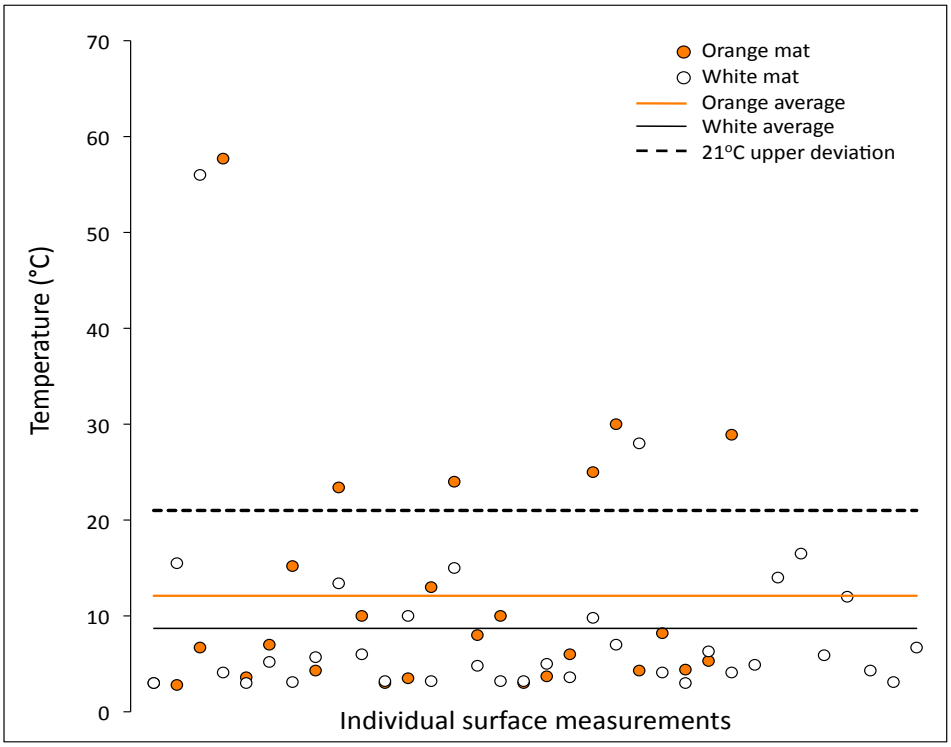

Figure 4. Individual temperature readings in orange and white *Beggiatoa* mats at the sediment surface of 60 temperature profiles. The lines indicate the temperature average for orange (12.1°C) and white *Beggiatoa* mats (8.7°C). Although most datapoints are in the low temperature range (<10°C), some high temperature measurements above the upper extent of standard deviation from the mean (21°C) are present, and are found more frequently in orange *Beggiatoa* mats than in white mats.

greater thermotolerance than white *Beggiatoa*. As a caveat, our data represent one-time snapshots of *Beggiatoa* communities that move and rearrange in response to a dynamic hydrothermal system, and we cannot be sure whether outliers represent temporary surges or sites where elevated hydrothermal flux is more persistent. Daily photo surveys of a *Beggiatoa* mat on our 2009 cruise demonstrated subtle but noticeable changes in surface texture over 11 days, which could indicate rapid fluctuations in subsurface hydrothermal flow. Moreover, a well-developed *Beggiatoa* mat with subsurface temperatures of 50°C

(Marker 6) was documented during our 2008 cruise, but had disappeared in 2009; only bare sediment with a subsurface temperature (at 40 cmbsf) of less than 6°C was found.

While surface temperatures illuminate *in situ* temperature ranges of Guaymas *Beggiatoa* spp., subsurface temperatures provide information related to the strength of hydrothermal flow beneath the mat. The average temperatures at 40 cmbsf from groups O and W are not significantly different from one another, but both are significantly warmer than average temperatures below bare sediments, in groups S and B (Figure 3). These observations are consistent with our working hypothesis that hydrothermal activity and temperatures are higher beneath mat cover than beneath bare sediments, whether bare sediments are near or far from a mat. The average 40 cmbsf-temperatures for all 15 mats *with orange and white Beggiatoa* do not suggest a predictive relationship between filament color and subsurface temperature (Figure 3), in the sense that a particular subsurface temperature should always correspond to a specific *Beggiatoa* color. Temperature regimes change considerably from one mat to the next, and temperature ranges beneath *Beggiatoa* of the same color but from different mats can be distinct from one another.

During dives 4483, 4490, 4569, and 4572 temperature, sulfide, and sulfate profiles were taken in transects across four separate orange and white *Beggiatoa* mats, allowing unambiguous color groupings in close proximity for optimal comparison (Figure 5). Mats from dives 4483, 4490, 4569, and 4572 will now be referred to as Mats 1, 2, 3, and 4, respectively. All surface temperatures from Mats 1, 2, and 3 are 3°C except in the orange portion of Mat 3, which at 13°C remains within the expected range of surface temperatures in *Beggiatoa* mats (see above), while all subsurface temperatures

increase with depth (Figure 5A). Surface temperatures from mat 4 are not available but subsurface temperatures do increase with depth. Temperature profiles taken in bare sediments with no mat cover yield the coolest temperatures. Next to Mats 1 and 2, the bare sediment profiles at 10 cm distance from mat cover were warmer than the temperature profiles next to mats 3 and 4, at 25 and 15 cm distance, respectively. This is consistent with our prediction that elevated temperatures due to hydrothermal activity decrease with increasing distance from *Beggiatoa* mats.

Transects of temperature profiles for individual mats show that the typical sequence of orange and white *Beggiatoa* mats are supported by hydrothermal fluid of different temperatures (Figure 5A). Orange filaments in mats 1, 2 and 3 are positioned over the shallow subsurface temperature maximum (at 40 cmbsf) and are surrounded by white mats overlying less hot sediments. At the same time, there are no predictive temperature regimes for orange versus white mats, since the temperature ranges associated with white or orange *Beggiatoa* can shift from one mat to another. For example, at 40 cm sediment depth, the temperature regimes below *Beggiatoa* filaments of the same color in Mats 1 and 3 are 15-30°C lower than in their Mat 2 counterparts, even though the subsurface temperature distribution of orange and white *Beggiatoa* in relation to each other remains the same. Mat 4 provides an interesting exception: here, the temperature profile underneath white *Beggiatoa* is initially cooler than the orange mat-associated temperature profile, but it steepens downcore, and surpasses the temperature of the orange profile at a depth of 25 cmbsf. These temperature curves could result from lateral fluid flow, where the hottest fluid passes sideways or at an angle underneath the

white mat before it approaches the sediment surface laterally offset underneath the orange mat.

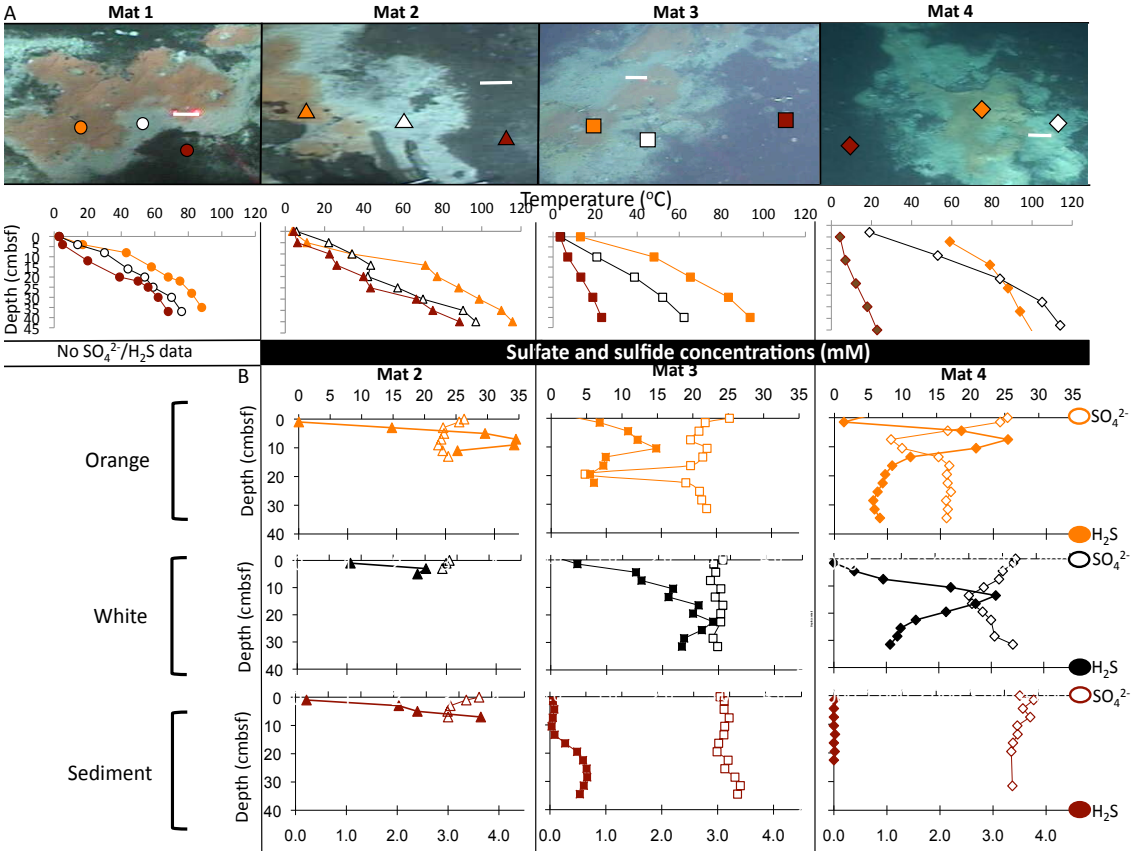

Figure 5A. Temperature profiles from four selected *Beggiatoa* mats for comparison of temperature regimes along gradients from orange mat to white mat to nearby sediments. **Mat 1)** *Beggiatoa* mat at Marker 2, Dive 4483, Dec 6, 2008 (27°N0.463, 111°W24.556). **Mat 2)** *Beggiatoa* mat ca. 25 m southwest of Megamat, Dive 4490, Dec 14, 2008 (27°N0.446, 111°W24.532). **Mat 3)** *Beggiatoa* mat at Marker 14, Dive 4569, Nov. 30, 2009 (27°N0.47, 111°W24.431). **Mat 4)** *Beggiatoa* mat at Marker 27, Dive 4572, Dec. 2, 2009 (27°N0.445, 111°W24.529).
5B) Sulfate and sulfide profiles from Mats 2, 3, and 4 for comparison of geochemical regimes along gradients from orange mat to white mat to nearby sediments.

If temperature provides an applicable proxy, hydrothermal fluid flow may be greater to the orange portions than to the white portions of *Beggiatoa* mats. Although a definitive calculation of hydrothermal flux cannot be achieved from the current dataset, Fourier's law for the transfer of heat demonstrates the tendency of a heat flux, whether conductive, convective, or a combination of both, to (i) increase with the magnitude of a gradient and (ii) be in a direction opposite the direction of the gradient. As such, higher

temperature gradients imply higher heat fluxes. Because hydrothermal fluids are both a source of heat and of reduced organic and inorganic compounds to surface sediments, an increase in heat flux implies a related increase in delivery of electron donors and carbon sources to the *Beggiatoa* living at the sediment-water interface. Higher temperature gradients exist beneath the orange portions of three out of four mats, and temperature profiles below bare sediments are lowest for all four mats. Thus, it appears that within a given mat, orange *Beggiatoa* filaments usually concentrate over the local hydrothermal flux maximum and may therefore receive the greatest supply of carbon sources and metabolically relevant electron donors like sulfide. However, this interpretation might be too simplistic for two reasons. First, temperature and microbial substrate flux supporting mat growth may not always be proportionally linked; substantial variation may be caused by localized cooling of vent fluids, temporal changes in fluid flow, or subsurface microbial activity levels. Second, temperature and hydrothermal flux maxima could impact *Beggiatoa* mats indirectly, by pushing subsurface anaerobic remineralization and respiration processes that produce sulfide and other electron donors towards the surface sediments.

These possibilities were investigated by measuring porewater sulfate and sulfide concentrations in the shallow subsurface. The sulfide profiles and peaks result from the interplay of upwardly or laterally migrating sulfidic subsurface fluid, biogenic sulfate reduction fuelled by low-molecular-weight carbon substrates within the sediment, and sulfide oxidation near the sediment surface where suitable electron acceptors such as oxygen and nitrate are available. For Mats 2, 3, and 4, push cores for porewater analysis, including sulfide and sulfate, were retrieved next to the temperature profiles (Figure 5B).

First, the results show a linkage between high subsurface temperatures and increased sulfide concentrations. The maximum sulfide concentration ranged between 2 mM and 3 mM beneath the orange and white sections of all three mats. Sulfide concentrations beneath the orange and white portions of Mats 3 and 4 are substantially greater than the sulfide concentrations beneath the bare sediment portions near the same mats. These enhanced sulfide concentrations are congruent with the temperature profiles of these mats, which show that bare sediment subsurface temperatures are substantially lower—not surpassing 20°C at depth—than the orange and white subsurface temperatures, which reach at least 60°C at depth. If mat cover, high temperature, and sulfide concentration are always linked, bare sediments without mats should be cold and contain no sulfide. However, the bare sediment in Mat 2 gives an example that such sites can have a high sulfide supply and hot temperatures. We hypothesize that sulfidic, hydrothermally active bare sediment sites undergo gradual *Beggiatoa* mat colonization, and time series studies would provide an answer to this question.

Second, the sulfide profiles are consistent with microbial activity zones in the shallow subsurface that shift vertically in response to the temperature regime. The two processes that generate and consume porewater sulfide—sulfate reduction and sulfide oxidation—are temperature-dependent. Microbial sulfide oxidation becomes thermodynamically unfavorable at temperatures above 50°C (McCollom and Shock, 1997), and temperatures from 90 – 100°C constitute the upper limit for reliably detected microbial sulfate reduction in Guaymas Basin sediments (Jørgensen et al., 1990; Elsgaard et al., 1994; Weber and Jørgensen, 2002). Consequently, hotter temperature profiles compress the dominant zones of each metabolism towards the sediment surface where

temperatures are cooler. This is seen in Mat 3 and Mat 4, where the shallowest sulfide concentration maxima coincide with hotter temperature regimes below the orange portion of the mats. Beneath the white sections of Mats 3 and 4, the sulfide maxima are not only deeper, but the profiles are stretched across a greater depth range. Consistent with this interpretation, the sulfide maxima in Mats 3 and 4 coincide with temperatures of 40 – 60°C, around the upper limit for sulfide oxidation (McCollom and Shock, 1997) and also near the upper growth limit for sulfide-oxidizing ε-proteobacteria (Campbell et al., 2006), the most commonly found sulfur oxidizers at hydrothermal vents including Guaymas Basin (Teske et al., 2002). Moreover, 50°C, the temperature at which sulfate reduction rates in Guaymas sediments are highest (Jørgensen et al., 1990) falls within this range. At lower temperatures towards the sediment surface, sulfide oxidation removes sulfide faster than sulfate reduction produces it; at higher temperatures in deeper sediments, sulfide generation by thermophilic sulfate reduction prevails.

Thus, the distribution pattern of orange and white *Beggiatoa* may be a consequence of temperature- and hydrothermal flux-driven upward compression of metabolic zones in the sediments underneath the mats, and the associated steeper fluxes of metabolic products, including sulfide, that are generated in the near-surface sediment and transported to the sediment surface where the *Beggiatoa* mat resides. A variation of the Guaymas model, where electron acceptor limitation replaces temperature as the primary influence that compresses metabolic zones, provides a working hypothesis for the same spatial distribution of orange and white *Beggiatoa* filaments in cold hydrocarbon seep sediments in the Gulf of Mexico (Larkin and Henk, 1996; Nikolaus et al., 2003). Here, the upward flux of anoxic, sulfate-free subsurface fluid sustains and at

the same time compresses the zone of highest sulfate reduction rates towards the mat-covered sediment surface (Lloyd et al. 2010). To summarize, we suggest that (i) the subsurface temperature regime that results from localized hydrothermal flux in Guaymas Basin drives and compresses metabolic activity towards the sediment surface, and (ii) the resulting increased supply of reducing compounds and energy sources to *Beggiatoa* mats at the sediment surface controls the differential positioning of orange and white *Beggiatoa* filaments.

Supposing our interpretation of this system is accurate and flux of energy sources is greatest to the predominantly orange center of the mat, a possible explanation for this is that orange *Beggiatoa* filaments have a smaller capacity than white filaments for storage of electron donor in the form of elemental sulfur, and therefore cannot persist as long as white filaments during periods of inadequate sulfide delivery. This is consistent with the observation that white filaments typically fall within the largest width group, ~120 μm, while orange filaments are classified into the two smaller width classes of ~25 μm and ~35 μm. Although we know little concerning the volume of the thin cytoplasmic layer where elemental sulfur is stored, a large white filament is likely to have more storage space than a thin orange filament. This could also explain why some white filaments were found in the orange portions of mats and no orange filaments were observed in the white sections, as white filaments may have the ability to grow further from the direct hydrothermal source than orange filaments. However, depending on the ratio of cytoplasmic volume to total biomass, an increase in electron donor storage space might also mean a relative increase in biomass to support. Further studies to assess the thickness of the cytoplasmic layer, such as freeze-fracture and transmission electron

microscopy (Costello 2006; Larkin and Henk 1996), or direct concentration measurements of elemental sulfur stored within filaments (Zopfi et al., 2001), are needed to determine a Beggiatoa filament's capacity for storage of electron donors.

Conclusion

The as-yet uncultivated *Beggiatoa* spp. at Guaymas Basin represent at least five separate phylotypes and colonize the surface of hydrothermal sediments in contact with seawater at about 3°C. Temperatures at the *Beggiatoa*-inhabited sediment-water interface usually range between 3 and 16°C but may reach as much as 60°C, while surface temperatures of non-*Beggiatoa* inhabited sediments are typically nearer ambient seawater temperatures of 3-4°C. Because *in situ* temperature peaks were observed more frequently in orange mat areas than in white mat areas, we suggest that orange filaments may be more thermotolerant than white filaments, but further studies are necessary to confirm this.

Within a given mat, orange *Beggiatoa* spp. are usually restricted to surface sediments above the steepest subsurface temperature gradients as well as more compressed sulfide concentration profiles. We conclude that the delivery rate of, and proximity to electron sources in the microbially active shallow subsurface, rather than the *in situ* temperature range by itself, controls the differential positioning of orange and white filaments in a *Beggiatoa* mat. Future work will integrate functional-gene sequencing of orange and white *Beggiatoa* filaments, geochemical characterization of

sulfide, dissolved inorganic carbon and organic acid gradients, and *in situ* temperature logger data that document temperature fluctuations and *Beggiatoa* mat response over several days.

Appendix I: Table 1

A. The upper sections (-5 – 20 cmbsf) of all temperature profiles

Profiles highlighted in grey are from *Beggiatoa* mats with only white filaments (where no orange filaments were detected).

Dive-Profile	Year	Location	-5	0	2	4	5	8	10	12	15	16	20
4483-HT1	2008	Orange mat		3		14				35			55
4483-HT1a	2008	Orange mat		2.8		17		43			58		68
4489-HF4	2008	Orange mat									34		
4489-HF8	2008	Orange mat		6.7					58				91.6
4489-HF9	2008	Orange mat		57.7					96				104
4490-HF1	2008	Orange mat	3.2	3.6			11		33.8		71.3		77.3
4492-HF3	2008	Orange mat		7					54				127
4493-HF2	2008	Orange mat		15.2					33.1				36
4493-HF3	2008	Orange mat		4.3					28.9				59.2
4493-HF4	2008	Orange mat		23.4					85.4				91.7
4493-HF6	2008	Orange mat		10					38				85
4483-HT2a	2008	Orange mat		3		12				36		54	
4483-HF1	2008	Orange mat	2.8	3.7					30				67
4483-HF3	2008	Orange mat	3	6					34				27
4483-HF4	2008	Orange mat	3	25					87				100
4483-HF7	2008	Orange mat	3	30					19				27
4485-HF7	2008	Orange mat		4.3					9.5				41.5
4485-HF14	2008	Orange mat	X										
4489-HF2	2008	Orange mat			11.3					37.2			
4489-HF3	2008	Orange mat		8.2					36.8				39.5
4490-HF2	2008	Orange mat	3.4	4.4			20.9		36.9		50.1		62.6
4568-INS1-HF5	2009	Orange mat		5.3					61.5				85.5
4573-M24-HF1	2009	Orange mat		28.9			91.3		103.1		96.7		77.2
4563-M14-HF4	2009	Orange mat		3.0					10.0				27.0
4568-INS1-HF3	2009	Orange mat		3.5			16.7		16.4		84.7		85.4
4569-M14-HF3	2009	Orange mat		13.0					48.0				65.3

Dive-Profile	Year	Location	-5	0	2	4	5	8	10	12	15	16	20
4562-WMM-HT1	2009	Orange mat		24.0									
4562-WMM-HT2	2009	Orange mat		8.0									
4562-WMM-HT3	2009	Orange mat		10.0									
4483-HT3a	2008	White mat		3		14		30				44	54
4483-HF8	2008	White mat	3	15.5					80.3				81.1
4483-HF2	2008	White mat	3	56					94				95
4483-HT1b	2008	White mat		6		105						107	106
4483-HT4b	2008	White mat		3		37			103				109
4483-HT5b	2008	White mat		15				64		95			107
4483-HF9	2008	White mat	2.8	54					99				105
4484-HF1	2008	White mat		21					119				134
4484-HF4	2008	White mat		3			14				35		
4484-HT1	2008	White mat		1.8				39		61		84.4	98
4485-HF8	2008	White mat		4.1					20.2				116.4
4485-HF13	2008	White mat	7				55.9				155.1		
4485-HF17	2008	White mat		3					15.7				45.7
4485-HF18	2008	White mat		5.2					37				68
4485-HF19	2008	White mat		3.1					7.5				30
4486-HT3	2008	White mat		3		57						101	130
4486-HF6	2008	White mat			55					111			
4490-HF3	2008	White mat	3.6	5.7			22.1		34		43.5		42
4490-HF6	2008	White mat	4.3	13.4			48.6		73.3		87.4		100.2
4490-HF7	2008	White mat		2					15				64
4492-HF2	2008	White mat		6					50				76
4493-HF1	2008	White mat		3.2					11				15
4493-HF5	2008	White mat		10					57.3				95.6
4483-HT4a	2008	White mat		3		16				28		41	51
4483-HF5	2008	White mat	3	6.3					29				44
4483-HF6	2008	White mat	3	4.1					19				36
4483-HT2b	2008	White mat		6				16		29			40

Dive-Profile	Year	Location	-5	0	2	4	5	8	10	12	15	16	20
4483-HT3b	2008	White mat		3		10				18			28
4483-HF10	2008	White mat	3	4.9					21				36
4484-HT2	2008	White mat						16.6		31.8		36.5	38.5
4485-HF	2008	White mat	2.94	4.9			9.5		39.5		58.9		75.6
4485-HF1	2008	White mat	4.1				16.8				39.9		
4485-HF2	2008	White mat	3.4	14			20.8		36		59.2		75.8
4485-HF3	2008	White mat	3.4	16.5			30.9		51.2		77.4		100.9
4485-HF4	2008	White mat	3.2	5.9			30.5		39.3		73.4		84.6
4485-HF5	2008	White mat	3.2	12			15.2		37.3		48.6		62.5
4485-HF6	2008	White mat	4				6.3				19.8		
4485-HF9	2008	White mat	5.5				34				119.1		
4485-HF10	2008	White mat	3.5				19.4				50.2		
4485-HF12	2008	White mat					7.6				21		
4485-HF15	2008	White mat	3.2				35.6				69.7		
4486-HF7	2008	White mat			31					68			
4489-HF5	2008	White mat		6.2					63				104
4489-HF6	2008	White mat		3.3					25				56.9
4489-HF7	2008	White mat		5.4					35.4				70
4490-HF4	2008	White mat	3.4	4.3			25.3		31.9		45.9		46
4491-HF1	2008	White mat		3.1					8.7				18.5
4491-HF4	2008	White mat		3					67				126
4491-HF5	2008	White mat		6					94				82
4491-HF6	2008	White mat		4									
4491-HF7	2008	White mat		4					26				57
4562-M1-HF1	2009	White mat		5.6			24.6		34.6		52.0		60.1
4562-M1-HF2	2009	White mat		3.9			24.7		23.9		50.4		64.4
4562-M1-HF6	2009	White mat		4.5			18.7		29.5		44.9		54.1
4563-M6-HF3	2009	White mat		3.2					6.5				36.6
4564-M27-HF1	2009	White mat		15.0					28.5				54.5
4564-M27-HF2	2009	White mat		55.0					77.6				95.7
4564-M27-HF3	2009	White mat		4.8					29.7				52.0

Dive-Profile	Year	Location	-5	0	2	4	5	8	10	12	15	16	20
4568-INS1-HF1	2009	White mat		3.2			13.7		23.7		45.1		56.6
4568-INS1-HF2	2009	White mat		3.2			13.1		17.5		43.1		43.6
4568-INS1-HF4	2009	White mat		5.0					16.4				47.3
4569-M14-HF2	2009	White mat		3.6					20.8				38.7
4569-INS1-HF1	2009	White mat		23.4					57.9				91.6
4569-INS1-HF3	2009	White mat		15.1					47.5				69.0
4569-INS1-HF4	2009	White mat		9.8					56.1				92.4
4569-M3-HF1	2009	White mat		7.0					20.6				34.7
4571-M4-HF3	2009	White mat		28.0					61.0				85.0
4573-M24-HF4	2009	White mat		4.1			28.1		37.1		64.7		68.5
4562-M1-HF3	2009	White mat		8.0			24.0		36.8		48.9		59.8
4562-M1-HF4	2009	White mat		7.0			16.3		25.9		37.5		47.4
4563-M6-HF2	2009	White mat		3.1					3.1				21.0
4569-M3-HF2	2009	White mat		6.7					13.8				28.2
4483-HT5a	2008	<1m Sediment		3		5				20			39
4485-HF	2008	<1m Sediment	2.92	2.95			2.88		2.88		2.96		3.01
4485-HF	2008	<1m Sediment	2.93	2.93			2.83		2.91		3.16		3.43
4485-HF16	2008	<1m Sediment	3	5.8			10.2		26.7		31.6		48
4486-HT1	2008	<1m Sediment		3		16		31				45	61
4486-HT2	2008	<1m Sediment		3		27				52			73
4486-HF4	2008	<1m Sediment			10					36			
4486-HF5	2008	<1m Sediment			14					39			
4486-HF8	2008	<1m Sediment			22					47			
4486-HF9	2008	<1m Sediment			16					47			
4486-HF10	2008	<1m Sediment			23					44			
4486-HF11	2008	<1m Sediment			24					40			
4490-HF5	2008	<1m Sediment	3	4.3			6.2		22.5		26.2		39.8
4490-HF8	2008	<1m Sediment		3.2					20.1				45.1
4491-HF3	2008	<1m Sediment		3					5				10
4492-HF1	2008	<1m Sediment		7					24				37

Dive-Profile	Year	Location	-5	0	2	4	5	8	10	12	15	16	20
4562-M1-HF5	2009	<1m Sediment		3.3			6.9		11.8		17.5		20.6
4571-M4-HF1	2009	<1m Sediment		6.9					27.7				43.7
4571-M4-HF2	2009	<1m Sediment		13.7					31.5				40.1
4572-M27-HF3	2009	<1m Sediment											
4485-HF	2008	>1m Background	2.94	2.95			2.84		2.87		2.93		2.95
4485-HF	2008	>1m Background	2.92	2.93			2.86		2.86		2.93		2.94
4491-HF2	2008	>1m Background		2.99					2.85				2.99
4562-M6-HF1	2009	>1m Background		3.2					3.4				3.8
4564-HF1	2009	>1m Background		4.8			5.2		8.9		9.9		14.2
4567-HF1	2009	>1m Background							3.2				3.4
4569-M14-HF1	2009	>1m Background		3.3					7.0				13.2
4569-YM-HF2	2009	>1m Background		2.9					2.9				2.9
4569-HF1	2009	>1m Background		2.9					2.9				2.9

B. The lower sections (22 – 55 cmbsf) of all temperature profiles

Profiles highlighted in grey are from *Beggiatoa* mats with only white filaments (where no orange filaments were detected).

Dive-Profile	22	24	25	28	30	32	35	37	40	42	45	55
4483-HT1		71				82						
4483-HT1a	75			82			88					
4489-HF4			54				60				64	65
4489-HF8					105				110			
4489-HF9					102				104			
4490-HF1			88.28		98.7		110		115.7			
4492-HF3					149				164			
4493-HF2					40.9				49			
4493-HF3					80.1				90.4			
4493-HF4					84.6				90.3			
4493-HF6					94				83			

Dive-Profile	22	24	25	28	30	32	35	37	40	42	45	55
4483-HT2a	64		70		75			80				
4483-HF1					91				96			
4483-HF3					24				18			
4483-HF4					102				101			
4483-HF7					43				37			
4485-HF7					120							
4485-HF14												
4489-HF2	41.8					43.2				44.4		
4489-HF3					41				40.8			
4490-HF2			76.8		89.2		98		105			
4568-INS1-HF5					90.7				96.4			
4573-M24-HF1			68.5		57.8		68.0		86.4		91.4	
4563-M14-HF4					43.0				54.0			
4568-INS1-HF3			98.3		96.5		100.3		99.6		103.6	
4569-M14-HF3					83.4				93.7			
4562-WMM-HT1												
4562-WMM-HT2												
4562-WMM-HT3												
4483-HT3a			59		70			76				
4483-HF8					85.6				94.1			
4483-HF2					97				100			
4483-HT1b			107			107						
4483-HT4b		109				109						
4483-HT5b				107			107					
4483-HF9					108				107			
4484-HF1					152				162			
4484-HF4			55				71		82			
4484-HT1		104.9			107.1		108.1	109.2				
4485-HF8					149.8							
4485-HF13			189.9				198.9		201.8			

Dive-Profile	22	24	25	28	30	32	35	37	40	42	45	55
4485-HF17					73.2				96.2			
4485-HF18					95.7				122.4			
4485-HF19					66.3				106.5			
4486-HT3		155		161			164	165				
4486-HF6	142					163				163		
4490-HF3			57.2		70.1		90.5		97			
4490-HF6			102.6		103.7		101.1		101.5			
4490-HF7					105				138			
4492-HF2					86				90			
4493-HF1					17				33			
4493-HF5					125.9				131.21			
4483-HT4a		60			66			72				
4483-HF5					48				67			
4483-HF6					52				60			
4483-HT2b			44	46		47						
4483-HT3b		33		34		35						
4483-HF10					45				51			
4484-HT2		39			35.8		28.8	21.6				
4485-HF			85.9		91		89.1		93.3			
4485-HF1			72.4									
4485-HF2			89.8		113.7		121.3		133.7			
4485-HF3			115.9		120.5		123.5		130.6			
4485-HF4			93.2		108.2		111.3		119.5			
4485-HF5			66.5		80.7		83.9		98.2			
4485-HF6			23				39.3					
4485-HF9			131.1				133		134.5			
4485-HF10			65.2				80.4					
4485-HF12			46.3									
4485-HF15												
4486-HF7	97					122				138		
4489-HF5					137				160			

Dive-Profile	22	24	25	28	30	32	35	37	40	42	45	55
4489-HF6					87.7				116			
4489-HF7					92				118			
4490-HF4			72.1		79.1		91.3		95.8			
4491-HF1					27.4				41.3			
4491-HF4					146				183			
4491-HF5					125				130			
4491-HF6									110			
4491-HF7					90				112			
4562-M1-HF1			74.7		81.5		94.0		99.9		111.0	
4562-M1-HF2			75.2		86.6		95.7		105.7		113.0	
4562-M1-HF6			68.8		77.5		89.0		95.8		104.5	
4563-M6-HF3					34.0				15.0			
4564-M27-HF1					70.2				104.0			
4564-M27-HF2					107.6				102.0			
4564-M27-HF3					74.0				88.0			
4568-INS1-HF1			78.6		88.6		102.3		108.6		115.0	
4568-INS1-HF2			81.3		90.0		98.1		102.6		103.9	
4568-INS1-HF4					95.0				96.7			
4569-M14-HF2					52.1				62.3			
4569-INS1-HF1					110.1				118.0			
4569-INS1-HF3					95.0				116.0			
4569-INS1-HF4					119.4				151.3			
4569-M3-HF1					49.8				58.0			
4571-M4-HF3					105.0				129.0			
4573-M24-HF4			78.2		78.6		82.3		82.7		86.5	
4562-M1-HF3			68.0		76.5		82.5		91.5		98.5	
4562-M1-HF4			59.3		68.1		78.0		84.3		93.6	
4563-M6-HF2					34.0				36.0			
4569-M3-HF2					32.5				36.5			
4483-HT5a	50		56		62			68				

Dive-Profile	22	24	25	28	30	32	35	37	40	42	45	55
4485-HF			3.12		3.25		3.27		3.45			
4485-HF			3.84		4.57		5.35		5.67			
4485-HF16			53.6		68		72.1		93.3			
4486-HT1				75		86		99				
4486-HT2		94		115		129		142				
4486-HF4	55					75				94		
4486-HF5	64					88				109		
4486-HF8	70					91				110		
4486-HF9	73					96				118		
4486-HF10	65					82				101		
4486-HF11	54					70				84		
4490-HF5			43.4		66.7		75.1		88.7			
4490-HF8					67.1				84.1			
4491-HF3					16				25			
4492-HF1					51				61			
4562-M1-HF5			32.1		36.7		48.8		54.3		64.8	
4571-M4-HF1					55.0				63.2			
4571-M4-HF2					45.3				49.7			
4572-M27-HF3												
4485-HF			2.99		3		2.97		2.97			
4485-HF			2.99		3.02		2.99		3.01			
4491-HF2					3.1				3.1			
4562-M6-HF1					4.6				5.5			
4564-HF1			15.5		22.0		22.5		27.0		28.6	
4567-HF1					3.6				3.8			
4569-M14-HF1					18.9				23.1			
4569-YM-HF2					3.0				3.0			
4569-HF1					2.9				2.9			

References

Campbell BJ, Engel AS, Porter ML, and Takai K (2006) The versatile epsilon-Proteobacteria: Key players in sulphidic habitats. *Nature Reviews Microbiology* **4**, 458–468.

Cline, JD (1969) Spectrophotometric determination of hydrogen sulfide in natural waters. *Limnology and Oceanography* **14**, 454-458.

Costello, MJ (2006) Cryo-electron microscopy of biological samples. *Ultrastructural Pathology* **30**, 361-371.

Dhillon A, Teske A, Dillon J, Stahl DA, Sogin ML (2003) Molecular Characterization of Sulfate-Reducing Bacteria in the Guaymas Basin. *Applied and Environmental Microbiology* **69**, 2765-2772.

Dhillon A, Lever M, Lloyd KG, Albert DB, Sogin ML, Teske A (2005) Methanogen diversity evidenced by molecular characterization of methyl coenzyme M reductase (*mcrA*) genes in hydrothermal sediments of the Guaymas Basin. *Applied and Environmental Microbiology.* **71**, 4592-4601.

Edmond JM, Von Damm K (1985) Chemistry of ridge crest hot springs. *Biological Society of Washington Bulletin* **6**, 43–47.

Einsele G, Gieskes JM, Curray J, Moore DM, Aguayo E, Aubry MP, Fornari D, Guerrero J, Kastner M, Kelts K, Lyle M, Matoba Y, Molina-Cruz A, Niemitz J, Rueda J, Saunders A, Schrader H, Simoneit B, Vacquier V (1980) Intrusion of basaltic sills into highly porous sediments, and resulting hydrothermal activity. *Nature* **283**, 441-445.

Elsgaard L, Isaksen MF, Jørgensen BB, Alayse AM, Jannasch HW (1994) Microbial sulfate reduction in deep-sea sediments at the Guaymas Basin hydrothermal vent area: Influence of temperature and substrates. *Geochimica et Cosmochimica Acta* **58**, 3335-3343.

Gundersen, JK, Jørgensen BB, Larsen E, Jannasch HW (1992) Mats of giant sulphur bacteria on deep-sea sediments due to fluctuating hydrothermal flow. *Nature* **360**, 454-456.

Jannasch HW, Nelson DC, Wirsen CO (1989) Massive natural occurrence of unusually large bacteria (*Beggiatoa* sp.) at a hydrothermal deep-sea vent site. *Nature* **342**, 834-836.

Jørgensen BB, Zawacki LX, Jannasch HW (1990) Thermophilic bacterial sulfate reduction in deep-sea sediments at the Guaymas Basin hydrothermal vents (Gulf of California). *Deep-Sea Research Part I* **37**, 695–710.

Kalanetra KM, Huston, SL, Nelson, DC (2004) Novel, attached, sulfur-oxidizing bacteria at shallow hydrothermal vents possess vacuoles not involved in respiratory nitrate accumulation. *Applied and Environmental Microbiology* **70**,7487-7496.

Larkin JM, Henk MC (1996) Filamentous Sulfide-Oxidizing Bacteria at Hydrocarbon Seeps of the Gulf of Mexico. *Microscopy Research and Technique* **33**, 23-31.

Lloyd KG, Albert DB, Biddle JF, Chanton JP, Pizarro O, Teske A (2010) Spatial Structure and Activity of Sedimentary Microbial Communities Underlying a *Beggiatoa* spp. Mat in a Gulf of Mexico Hydrocarbon Seep. *PLoS One* **5**, e8738.

Ludwig W, Strunk O, Westram R, Richter L, Meier H, et al. (2004) ARB: a software environment for sequence data. *Nucleic Acids Research* **32**, 1363-1371.

Martens CS, Albert DB, Alperin MJ (1999) Stable isotope tracing of anaerobic methane oxidation in the gassy sediments of Eckernförde Bay, German Baltic Sea. *American Journal of Science* **299**, 589–610.

McCollom TM, Shock EL (1997) Geochemical constraints on chemolithoautotrophic metabolism by microorganisms in seafloor hydrothermal systems. *Geochimica et Cosmochimica Acta* **61**, 4375–4391.

McHatton SC, Barry JP, Jannasch HW, Nelson DC (1996) High nitrate concentrations in vacuolate, autotrophic marine *Beggiatoa*. *Applied and Environmental Microbiology* **62**, 954-958.

Nelson DC, Wirsen CO, Jannasch HW (1989) Characterization of large, autotrophic *Beggiatoa* spp. abundant at hydrothermal vents of the Guaymas Basin. *Applied and Environmental Microbiology* **55**, 2909-2917.

Nikolaus R, Ammerman JW, MacDonald IR (2003) Distinct pigmentation and trophic modes in *Beggiatoa* from hydrocarbon seeps in the Gulf of Mexico. *Aquatic Microbial Ecology* **32**, 85-93.

Prince RC, Stokley KE, Haith CE, Jannasch HW (1988) The cytochromes of a marine *Beggiatoa*. *Archives of Microbiology* **150**, 193-196.

Pruesse E, Quast C, Knittel K, Fuchs B, Ludwig W, Peplies J, Glöckner FO (2007) SILVA: a comprehensive online resource for quality checked and aligned ribosomal RNA sequence data compatible with ARB. *Nucleic Acids Research* **35**, 7188-7196.

Schulz HN, Jørgensen BB (2001) Big Bacteria. *Annual Review of Microbiology* **55**, 105-137.

Teske A, Hinrichs K, Edgcomb V, Gomez A, Kysela D, Sylva SP, Sogin ML, Jannasch HW (2002) Microbial Diversity of Hydrothermal Sediments in the Guaymas Basin: Evidence for Anaerobic Methanotrophic Communities. *Applied and Environmental Microbiology* **68**, 1994-2007.

Teske A, Edgcomb V, Rivers AR, Thompson JR, Gomez A, Molyneaux SJ, Wirsen CO (2009) A molecular and physiological survey of a diverse collection of hydrothermal vent Thermococcus and Pyrococcus isolates. *Extremophiles* **13**, 905-915.

Von Damm KL, Edmond JM, Measures CI, Grant B (1985) Chemistry of submarine hydrothermal solutions at Guaymas Basin, Gulf of California. *Geochimica et Cosmochimica Acta* **49**, 2221–2237.

Weber A, Jørgensen BB (2002) Bacterial sulfate reduction in hydrothermal sediments of the Guaymas Basin, Gulf of California, Mexico. *Deep-Sea Research Part I* **49**, 827–841.

Zopfi J, Kjær T, Nielsen LP, Jørgensen BB (2001) Ecology of *Thioploca* spp.: nitrate and sulfur storage in relation to chemical microgradients and influence of *Thioploca* spp. on the sedimentary nitrogen cycle. *Applied and Environmental Microbiology* **67**, 5530-5537.